Evolution of microbial growth traits under serial dilution

Jie Lin,¹ Michael Manhart,^{2,3} and Ariel Amir¹ ¹ John A. Paulson School of Engineering and Applied Sciences, Harvard University, Cambridge, MA 02138, USA ²Department of Chemistry and Chemical Biology, Harvard University, Cambridge, MA 02138, USA ³Institute of Integrative Biology, ETH Zurich, 8092 Zurich, Switzerland (Dated: August 4, 2020)

Selection of mutants in a microbial population depends on multiple cellular traits. In serialdilution evolution experiments, three key traits are the lag time when transitioning from starvation to growth, the exponential growth rate, and the yield (number of cells per unit resource). Here we investigate how these traits evolve in laboratory evolution experiments using a minimal model of population dynamics, where the only interaction between cells is competition for a single limiting resource. We find that the fixation probability of a beneficial mutation depends on a linear combination of its growth rate and lag time relative to its immediate ancestor, even under clonal interference. The relative selective pressure on growth rate and lag time is set by the dilution factor; a larger dilution factor favors the adaptation of growth rate over the adaptation of lag time. The model shows that yield, however, is under no direct selection. We also show how the adaptation speeds of growth and lag depend on experimental parameters and the underlying supply of mutations. Finally, we investigate the evolution of covariation between these traits across populations, which reveals that the population growth rate and lag time can evolve a nonzero correlation even if mutations have uncorrelated effects on the two traits. Altogether these results provide useful guidance to future experiments on microbial evolution.

sis [5], the distribution of selection coefficients from sponof adaptive genomic variants [8], and the preponderance of clonal interference [9]. Despite this progress, links between the selection of mutations and their effects on specific cellular traits have remained poorly characterized. Growth traits — such as the lag time when transitioning from starvation to growth, the exponential growth rate, and the yield (resource efficiency) — are ideal candidates for investigating this question. Their association with growth means they have relatively direct connections to selection and population dynamics. Furthermore, highthroughput techniques can measure these traits for hundreds of genotypes and environments [10–13]. Numerous experiments have shown that single mutations can be pleiotropic, affecting multiple growth traits simultaneously [14, 15]. More recent experiments have even mea-29 sured these traits at the single-cell level, revealing substantial non-genetic heterogeneity [10, 13, 16]. Several evolution experiments have found widespread evidence of adaptation in these traits [17–20]. This data altogether indicates that covariation in these traits is pervasive in microbial populations.

There have been a few previous attempts to detraits. For example, Vasi et al. [17] considered data af-

Laboratory evolution experiments in microbes have 42 either fix, go extinct, or coexist. Wahl and Zhu [22] stud-10 provided insight into many aspects of evolution [1-3], 43 ied the fixation probability of mutations affecting differ-11 such as the speed of adaptation [4], the nature of epista- 44 ent growth traits separately (non-pleiotropic), especially 45 to identify which traits were most likely to acquire fixed taneous mutations [6], mutation rates [7], the spectrum 46 mutations and the importance of mutation occurrence 47 time and dilution factor. However, simple quantitative 48 results that can be used to interpret experimental data 49 have remained lacking. More recent work [23, 24] de-50 rived a quantitative relation between growth traits and 51 selection, showing that selection consists of additive com-52 ponents on the lag and growth phases. However, this did 53 not address the consequences of this selection for evolu-54 tion, especially the adaptation of trait covariation.

In this work we investigate a minimal model of evolu-56 tionary dynamics in which cells interact only by compe-57 tition for a single limiting resource. We find that the 58 fixation probability of a mutation is accurately deter-59 mined by a linear combination of its change in growth 60 rate and change in lag time relative to its immediate an-61 cestor, rather than depending on the precise combination 62 of traits; the relative weight of these two components is 63 determined by the dilution factor. Yield, on the other 64 hand, is under no direct selection. This is true even in 65 the presence of substantial clonal interference, where the 66 mutant's immediate ancestor may have large a fitness 67 difference with the population mean. We provide quanvelop quantitative models to describe evolution of these 68 titative predictions for the speed of adaptation of growth 69 rate and lag time as well as their evolved covariation. ter 2000 generations of evolution in Escherichia coli to 70 Specifically, we find that even in the absence of an inestimate how much adaptation was attributable to differ- 71 trinsic correlation between growth and lag due to muta-40 ent growth traits. Smith [21] developed a mathematical 72 tions, these traits can evolve a nonzero correlation due 41 model to study how different traits would allow strains to 73 to selection and variation in number of fixed mutations.

MATERIALS AND METHODS

Model of population dynamics

75

We consider a model of asexual microbial cells in a well-mixed batch culture, where the only interaction between different strains is competition for a single limiting resource [23, 24]. Each strain k is characterized by a lag time L_k , growth rate r_k , and yield Y_k (see Fig. 1a for a two-strain example). Here the yield is the number of cells per unit resource [17], so that $N_k(t)/Y_k$ is the amount of 83 resources consumed by time t by strain k, where $N_k(t)$ 84 is the number of cells of strain k at time t. We define 85 R to be the initial amount of the limiting resource and 86 assume different strains interact only by competing for 87 the limiting resource; their growth traits are the same as when they grow independently. When the population 89 has consumed all of the initial resource, the population 90 reaches stationary phase with constant size. The sat g_1 uration time t_c at which this occurs is determined by $\sum_{\text{strain } k} N_k(t_c)/Y_k = R$, which we can write in terms of the growth traits as

$$\sum_{\text{strain } k} \frac{N_0 x_k e^{r_k (t_c - L_k)}}{Y_k} = R, \tag{1}$$

where N_0 is the total population size and x_k is the fre- $_{95}$ quency of each strain k at the beginning of the growth $_{96}$ cycle. In Eq. 1 we assume the time $t_{\rm c}$ is longer than 97 each strain's lag time L_k . Note that some of our notation differs from related models in previous work, some ₉₉ of which used g for growth rate and λ for lag time [23], while others used λ for growth rate [25]. Although it is possible to extend the model to account for additional 102 growth traits such as a death rate or lag and growth on secondary resources, here we focus on the minimal set of traits most often measured in microbial phenotyping $_{\scriptscriptstyle{118}}$ experiments [10–12, 14–16, 18, 26].

We define the selection coefficient between each pair of 107 strains as the change in their log-ratio over the complete 108 growth cycle [27, 28]:

$$s_{ij} = \ln\left(\frac{N_i^{\text{final}}}{N_j^{\text{final}}}\right) - \ln\left(\frac{N_i^{\text{initial}}}{N_j^{\text{initial}}}\right)$$
$$= r_i(t_c - L_i) - r_j(t_c - L_j), \tag{2}$$

where $N_i^{\rm initial}$ is the population size of strain i at the beginning of the growth cycle and $N_i^{\rm final}$ is the population $_{111}$ size of strain i at the end. After the population reaches 112 stationary phase, it is diluted by a factor of D into a fresh 129 where $\gamma = (r_2 - r_1)/r_1$ is the growth rate of the mutant medium with amount R of the resource, and the cycle 130 relative to the wild-type and $\omega = (L_2 - L_1)r_1$ is the rel-114 repeats (Fig. 1a). We assume the population remains 131 ative lag time. The approximation is valid as long as the 115 in the stationary phase for a sufficiently short time such 132 growth rate difference between the mutant and the wile-116 that we can ignore death and other dynamics during this 133 type is small (Supplementary Methods Sec. IV), which 117 phase [29, 30].

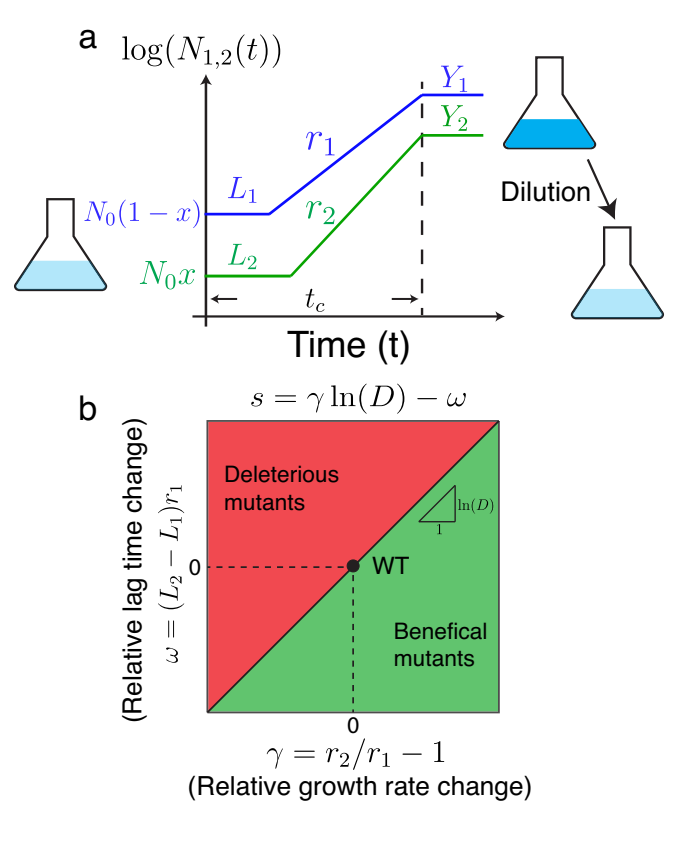


FIG. 1. Model of selection on multiple microbial growth traits. (a) Simplified model of microbial population growth characterized by three traits: lag time L, growth rate r, and yield Y. The total initial population size is N_0 and the initial frequency of the mutant (strain 2) is x. After the whole population reaches stationary phase (time t_c), the population is diluted by a factor D into fresh media, and the cycle starts again. (b) Phase diagram of selection on mutants in the space of their growth rate $\gamma = r_2/r_1 - 1$ and lag time $\omega = (L_2 - L_1)r_1$ relative to a wild-type. The slope of the diagonal line is $\ln D$.

Over many cycles of growth, as would occur in a laboratory evolution experiment [1, 28, 31], the population dynamics of this system are characterized by the set of frequencies x_k for all strains as well as the matrix of se-122 lection coefficients s_{ij} and the total population size N_0 123 at the beginning of each cycle. In Supplementary Meth-124 ods (Secs. I, II, III) we derive explicit equations for the 125 deterministic dynamics of these quantities over multiple 126 cycles of growth for an arbitrary number of strains. In the case of two strains, such as a mutant and a wild-type, 128 the selection coefficient is approximately

$$s \approx \gamma \ln D - \omega, \tag{3}$$

134 is true for most single mutations [6, 32]. This equation

135 shows that the growth phase and the lag phase make 186 We will assume mutational effects are not epistatic 136 distinct additive contributions to the total selection co- 187 and scale with the trait values of the background strain, efficient, with the dilution factor D controlling their rel- 188 so that $p_{\text{mut}}(r_2, L_2, Y_2 | r_1, L_1, Y_1) = p_{\text{mut}}(\gamma, \omega, \delta)$, where 138 ative magnitudes (Fig. 1b). This is because a larger 189 $\gamma = (r_2 - r_1)/r_1$, $\omega = (L_2 - L_1)r_1$, and $\delta = (Y_2 - Y_1)/Y_1$ 139 dilution factor will increase the amount of time the pop- 190 (Supplementary Methods Sec. V). Since our primary 140 ulation grows exponentially, hence increasing selection 191 goal is to scan the space of possible mutations, we fo-141 on growth rate. Neutral coexistence between multiple 192 cus on uniform distributions of mutational effects where 142 strains is therefore possible if these two selection com- 193 $-0.02 < \gamma < 0.02, -0.05 < \omega < 0.05$, and $-0.02 < \delta < 0.05$ ₁₄₃ ponents balance (s=0), although it requires an exact ₁₉₄ 0.02. In the Supplementary Methods we extend our main 144 tuning of the growth traits with the dilution factor (Sup- 195 results to the case of Gaussian distributions (Sec. V) 145 plementary Methods Sec. III) [23, 24]. With a fixed dilu-196 as well as an empirical distribution of mutational effects 146 tion factor D, the population size N_0 at the beginning of 197 based on single-gene deletions in E. coli (Sec. VI) [33]. 147 each growth cycle changes according to (Supplementary 148 Methods Sec. I):

$$N_0 = \frac{R\bar{Y}}{D},\tag{4}$$

where $\bar{Y}=(\sum_{\text{strain }k}x_k/Y_k)^{-1}$ is the effective yield of the whole population in the current growth cycle. In this manner the ratio R/D sets the bottleneck size of the 152 population, which for serial dilution is approximately the 153 effective population size [31], and therefore determines 154 the strength of genetic drift.

Model of evolutionary dynamics

155

157 mutations arise that alter growth traits. We start with 207 against their background strains, along with contours of 158 a wild-type population having lag time $L_0 = 100$ and 208 constant selection coefficient s from Eq. 3. As expected, ₁₅₉ growth rate $r_0 = (\ln 2)/60 \approx 0.012$, which are roughly ₂₀₉ fixed mutations either increase growth rate $(\gamma > 0)$, de-160 consistent with E. coli parameters where time is mea- 210 crease lag time ($\omega < 0$), or both. In contrast, the yield 161 sured in minutes [17, 31]; we set the wild-type yield to 211 of fixed mutations is the same as the ancestor on average $_{162}$ be $Y_0 = 1$ without loss of generality. As in experiments, $_{212}$ (Fig. 2b); indeed, the selection coefficient in Eq. 3 does we vary the dilution factor D and the amount of resources 213 not depend on the yields. If a mutation arises with sig-164 R, which control the relative selection on growth versus 214 nificantly higher or lower yield than the rest of the popsize of the first cycle to $N_0 = RY_0/D$.

Fig. 1a. Each cell division can generate a new mutation 219 yield have no effect on the overall population dynamics. ₁₇₃ erate a random waiting time τ_k for each strain k until the ₂₂₃ bination of traits, as long as other parameters such as 174 next mutation with instantaneous rate $\mu r_k N_k(t)$. When 224 the dilution factor D, the total amount of resource R, are drawn from a distribution $p_{\text{mut}}(r_2, L_2, Y_2 | r_1, L_1, Y_1)$, 226 Mathematically, this means that the fixation probability 179 are the traits for the new mutant. Note that since mu- 229 To test this, we discretize the scatter plot of Fig. 2a and 180 tations only arise during the exponential growth phase, 230 compute the fixation probabilities of mutations as func-₁₈₁ beneficial or deleterious effects on lag time are not real-₂₃₁ tions of γ and ω (Supplementary Methods Sec. VII). We 182 ized until the next growth cycle [20]. After the growth 232 then plot the resulting fixation probabilities of mutations 183 cycle ceases (once the resource is exhausted according to 233 as functions of their selection coefficients calculated by 184 Eq. 1), we randomly choose cells, each with probability 234 Eq. 3 (Fig. 2c,d,e,f). We test the dependence of the fixa- $_{185}$ 1/D, to form the population for the next growth cycle. $_{235}$ tion probability on the selection coefficient over a range

Data Availability

Data and codes are available upon request. File S1 200 contains the Supplementary Methods. File S2 contains 201 data of growth traits presented in Figure S3.

II. RESULTS

Fixation of mutations

We first consider the fixation statistics of new muta-205 tions in our model. In Fig. 2a we show the relative growth We now consider the evolution of a population as new 206 rates γ and the relative lag times ω of fixed mutations lag (set by D, Eq. 3) and the effective population size 215 ulation, the bottleneck population size N_0 immediately (set by R/D, Eq. 4). We also set the initial population 216 adjusts to keep the overall fold-change of the population $_{217}$ during the growth cycle fixed to the dilution factor DThe population grows according to the dynamics in 218 (Eq. 4). Therefore mutations that significantly change

with probability $\mu = 10^{-6}$; note this rate is only for muta- 220 Figure 2a also suggests that the density of fixed mutions altering growth traits, and therefore it is lower than 221 tations in the growth-lag trait space depends solely on the rate of mutations anywhere in the genome. We gen- 222 their selection coefficients, rather than the precise commutation occurs, the growth traits for the mutant 225 and the distribution of mutational effects are held fixed. where r_1, L_1, Y_1 are the growth traits for the background $\rho(\gamma, \omega)$ of a mutation with growth effect γ and lag effect strain on which the new mutation occurs and r_2, L_2, Y_2 228 ω can be expressed as $\phi(\gamma, \omega) = \phi(\gamma \ln D - \omega) \equiv \phi(s)$.

(6)

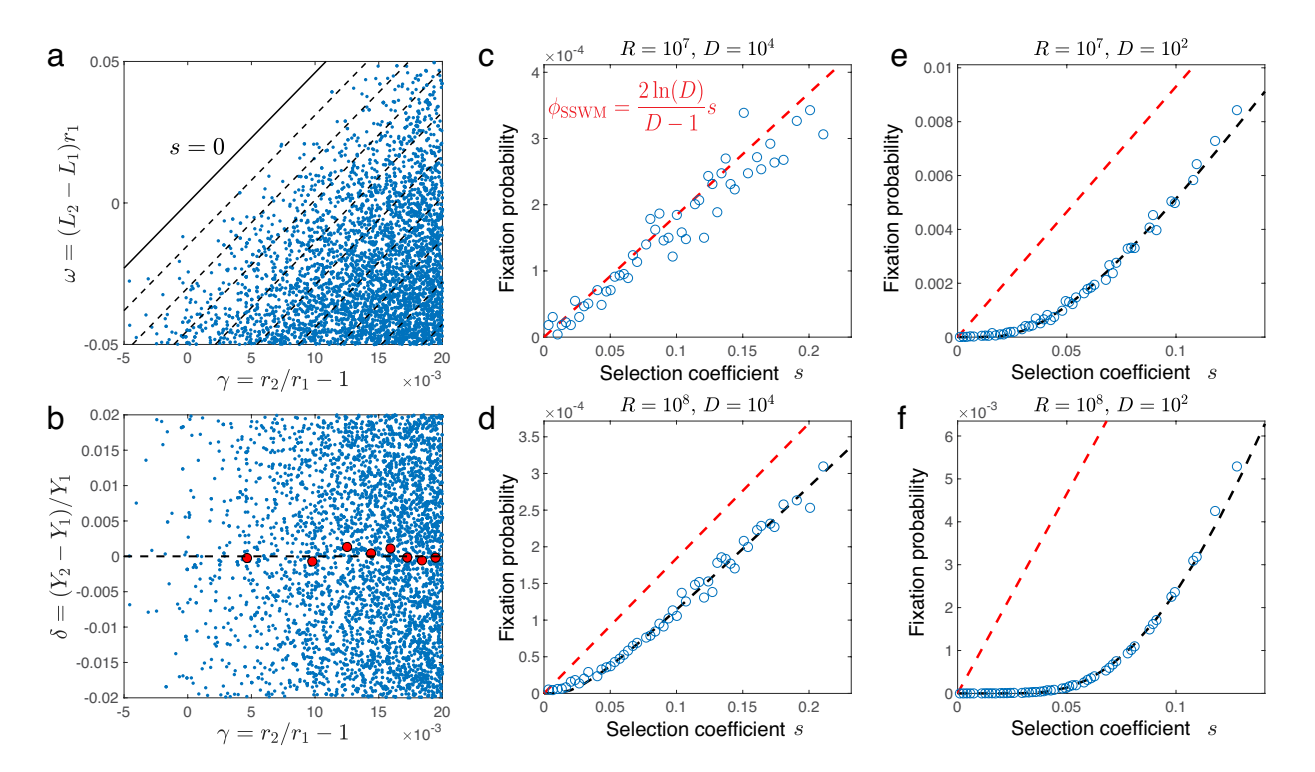


FIG. 2. Selection coefficient determines fixation probability. (a) The relative growth rates γ and the relative lag times ω of fixed mutations against their background strain. Dashed lines mark contours of constant selection coefficient with interval $\Delta s = 0.015$ while the solid line marks s = 0. (d) Same as (a) but for relative growth rate γ and the relative yield δ . The red dots mark the relative yield of fixed mutations averaged over binned values of the relative growth rate γ . In (a) and (d), $D=10^2$ and $R=10^7$. (b,c,e,f) Fixation probability of mutations against their selection coefficients for different amounts of resource R and dilution factors D as indicated in the titles. The red dashed line shows the fixation probability predicted in the SSWM regime (Eq. 5), while the black line shows a numerical fit of the data points to Eq. 6 with parameters A = 0.1145 and B = 0.0801 in (c), A = 0.0017 and B = 0.0421 in (e), and A = 0.2121 and B = 0.2192 in (f). In all panels mutations randomly arise from a uniform distribution p_{mut} with $-0.02 < \gamma < 0.02, -0.05 < \omega < 0.05$, and $-0.02 < \delta < 0.02$.

of population dynamics regimes by varying the dilution 256 mediate ancestor and not on the individual combination factor D and the amount of resources R.

mutation with selection coefficient s > 0 to be [22, 35, 36] 262 relation based on Gerrish and Lenski [38]:

257 of mutant traits (Fig. 2d,e,f), with all other population For small populations, mutations generally arise and 258 parameters held constant. Previous work has determined either fix or go extinct one at a time, a regime known as 259 the dependence of the fixation probability on the selec-"strong-selection weak-mutation" (SSWM) [34]. In this 260 tion coefficient under clonal interference using various apcase, we expect the fixation probability of a beneficial 261 proximations [38, 40-42]. Here, we focus on an empirical

$$\phi_{\text{SSWM}}(s) = \frac{2\ln D}{D-1}s. \tag{5}$$

small population size of $N_0 \sim R/D = 10^3$ (Fig. 2c). 255 selection coefficient (Eq. 3) relative to the mutation's im- 276 eficial mutations on the same background; Eq. 6 breaks

$$\phi_{\text{CI}}(s) = Ase^{-B/s},\tag{6}$$

where A and B are two constants that depend on other ²⁴³ This is similar to the standard Wright-Fisher fixation ²⁶⁴ parameters of the population (D, R, and the distribuprobability of 2s [37], but with a different prefactor due 255 tion of mutational effects); we treat these as empirical to averaging over the different times in the exponential 266 parameters to fit to the simulation results, although Gergrowth phase at which the mutation can arise (Supple- 267 rish and Lenski [38] predicted $A = 2 \ln D/(D-1)$, i.e., mentary Methods Sec. VIII). Indeed, we see this pre- 268 the same constant as in the SSWM case (Eq. 5). The dicted dependence matches the simulation results for the $_{269}$ $e^{-B/s}$ factor in Eq. 6 comes from the probability that no 270 superior beneficial mutations appears before the current For larger populations, multiple beneficial mutations 271 mutation fixes. Since the time to fixation scales as 1/s, will be simultaneously present in the population and in- 272 we expect the average number of superior mutations to terfere with each other, an effect known as clonal inter- 273 be proportional to 1/s (for small s). This approximation ference [38–43]. Our simulations show that, as for the 274 holds only for selection coefficients that are not too small SSWM case, the fixation probability depends only on the 275 and therefore are expected to fix without additional ben277 down for weaker beneficial mutations that typically fix 332 ing fitness trajectories are shown in Fig. 3b. To see how ²⁷⁸ by hitchhiking on stronger mutations [40]. Nevertheless, ³³³ different traits contribute to the fitness increase, we also 279 Eq. 6 matches our simulation results well for a wide range 334 calculate the average population traits at the beginning 280 of selection coefficients achieved in our simulations and 335 of each cycle; for instance, the average population growth Furthermore, the constant A we fit to the simulation data 337 expected from Eq. 3, the average growth rate increases 285

tional distributions of mutational effects $p_{\text{mut}}(\gamma,\omega,\delta)$ in 348 recent work from Baake et al. [45]. and an empirical distribution of mutational effects esti- 353 averaged change in the average growth rate per cycle: mated from single-gene deletions in E. coli (Fig. S3). In Fig. S4a we further test robustness by using the neutral phenotype (orthogonal to the selection coefficient) to quantify the range of γ and ω trait combinations that nevertheless have the same selection coefficient and fixa- 354 where the bracket denotes an average over replicate poption coefficient on growth alone is insufficient to determine fixation probability.

While the dependence of fixation probability on the 308 selection coefficient is a classic result of population genetics [44], the existence of a simple relationship here is nontrivial since, strictly speaking, selection in this model is not only frequency-dependent [23] (i.e., selection between two strains depends on their frequencies) but also includes higher-order effects [24] (i.e., selection between strain 1 and strain 2 is affected by the presence of strain 3). Therefore in principle, the fixation probability of a 316 mutant may depend on the specific state of the popula-317 tion in which it is present, while the selection coefficient 318 in Eq. 3 only describes selection on the mutant in com-319 petition with its immediate ancestor. However, we see 320 that, at least for the parameters considered in our simulations, these effects are negligible in determining the 322 eventual fate of a mutation.

Adaptation of growth traits

323

As Fig. 3a shows, many mutations arise and fix over the timescale of our simulations, which lead to predictable trends in the quantitative traits of the population. We 366 330 evolved and ancestral cells for one cycle, analogous to 370 large D); even though this prediction assumes the SSWM

larger population sizes $N_0 \sim R/D > 10^4$ (Fig. 2d,e,f). 336 rate at growth cycle n is $r_{\text{pop}}(n) = \sum_{\text{strain } k} r_k x_k(n)$. As is indeed close to the predicted value of $2 \ln D/(D-1)$, 338 (Fig. 3c) and the average lag time decreases (Fig. 3d) except in the most extreme case of $N_0 \sim R/D = 10^6$ 339 for all simulations. In contrast, the average yield evolves 340 without apparent trend (Fig. 3e), since Eq. 3 indicates Altogether Fig. 2 shows that mutations with differ- 341 no direct selection on yield. We note that, while the cells ent effects on cell growth — for example, a mutant that 342 do not evolve toward lower or higher resource efficiency increases the growth rate and a mutant that decreases 343 on average, they do evolve to consume resources more the lag time — can nevertheless have approximately the 344 quickly, since the rate of resource consumption (r_k/Y_k) same fixation probability as long as their overall effects 345 for each cell of strain k) depends on both the yield as on selection are the same according to Eq. 3. To test 346 well as the growth rate. Therefore the saturation time of the robustness of this result, we verify it for several addi- 347 each growth cycle evolves to be shorter, consistent with

²⁹⁴ the Supplementary Methods: a Gaussian distribution of ³⁴⁹ Figure 3 suggests relatively constant speeds of adapmutational effects, including the presence of correlated 350 tation for the relative fitness, the average growth rate, mutational effects (Fig. S1); a wider distribution of mu- 351 and the average lag time. For example, we can calculate tational effects with large selection coefficients (Fig. S2); 352 the adaptation speed of the average growth rate as the

$$W_{\text{growth}} = \langle r_{\text{pop}}(n+1) - r_{\text{pop}}(n) \rangle,$$
 (7)

tion probability, and in Fig. S4b we show that the selec- 355 ulations and cycle number. In the Supplementary Meth-356 ods (Secs. IX and X) we calculate the adaptation speeds 357 of these traits in the SSWM regime to be

$$W_{\text{growth}} = \sigma_{\gamma}^{2} r_{0}(\ln D) \left(\frac{\mu R Y_{0} \ln D}{D - 1}\right),$$

$$W_{\text{lag}} = -\frac{\sigma_{\omega}^{2}}{r_{0}} \left(\frac{\mu R Y_{0} \ln D}{D - 1}\right),$$

$$W_{\text{fitness}} = \frac{W_{\text{growth}}}{r_{0}} \ln D - W_{\text{lag}} r_{0},$$
(8)

358 where σ_{γ} and σ_{ω} are the standard deviations of the un- $_{359}$ derlying distributions of γ and ω for single mutations $p_{\text{mut}}(\gamma,\omega,\delta)$, p_{0} is the ancestral growth rate and p_{0} the 361 ancestral yield (we assume the yield does not change on 362 average according to Fig. 3e). Furthermore, the ratio of 363 the growth adaptation rate and the lag adaptation rate 364 is independent of the amount of resource and mutation 365 rate in the SSWM regime:

$$\frac{W_{\text{growth}}}{W_{\text{lag}}} = -r_0^2 \frac{\sigma_{\gamma}^2}{\sigma_{\omega}^2} \ln D. \tag{9}$$

Equation 8 predicts that the adaptation speeds of the first determine the relative fitness of the evolved pop- 367 average growth rate, the average lag time, and the relulation at each time point against the ancestral strain 368 ative fitness should all increase with the amount of reby simulating competition between an equal number of $_{369}$ sources R and decrease with the dilution factor D (for ₃₃₁ common experimental measurements [1, 31]. The result- ₃₇₁ regime (relatively small $N_0 \sim R/D$), it nevertheless holds

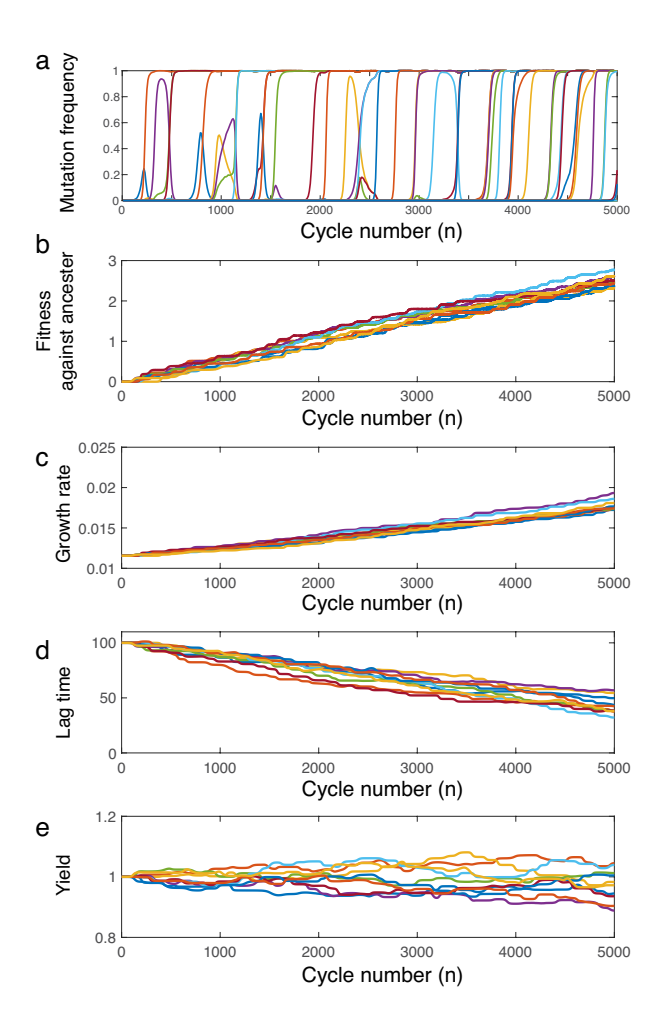


FIG. 3. Dynamics of evolving populations. (a) Frequencies of new mutations as functions of the number n of growth cycles. Example trajectories of (b) the fitness of the evolved population relative to the ancestral population, (c) the evolved average growth rate, (d) the evolved average lag time, and (e) the evolved average yield. In all panels the dilution factor is $D=10^2$, the amount of resource at the beginning of each cycle is $R = 10^7$, and mutations randomly arise from a uniform distribution p_{mut} with $-0.02 < \gamma < 0.02,\, -0.05 < \omega < 0.05,\,$ $^{\mbox{\tiny 418}}$ and $-0.02 < \delta < 0.02$.

across a wide range of R and D values (Fig. 4a,b,c), except for $R = 10^8$ where the speed of fitness increase is 374 non-monotonic with D (Fig. 4c). The predicted adapta-375 tion speeds in Eq. 8 also quantitatively match the simulated trajectories in the SSWM case (Fig. 4d,e,f); even 426 outside of the SSWM regime, the relative rate in Eq. 9 378 remains a good prediction at early times (Fig. S5).

Evolved covariation between growth traits

379

383 traits. Campos et al. [33] recently systematically measured the growth curves of the single-gene deletions in E. coli. We compute the relative growth rate, lag time, and yield changes for the single-gene deletions compared with the wild-type and find that the resulting empirical distribution of relative growth traits changes shows very small correlations between these traits (Fig. S3b,c), consistent with our assumptions. We note that these measurements, however, are subject to significant noise (Supplementary Methods Sec. VI), and therefore any conclusions ultimately require verification by further experiments.

Even in the absence of mutational correlations, selection may induce a correlation between these traits in evolved populations. In Fig. 5a we schematically depict how the raw variation of traits from mutations is distorted by selection and fixation of multiple mutations. Specifically, for a single fixed mutation, selection induces a positive (i.e., antagonistic) correlation between the relative growth rate change and the relative lag time change. 402 Figure 2a shows this for single fixed mutations, while 403 Fig. 5b,c shows this positive correlation between the average growth rate and the average lag time across populations that have accumulated the same number of fixed mutations. For populations in the SSWM regime with the same number of fixed mutations, the Pearson correlation coefficient between the average growth rate and the average lag time across populations is approximately equal to the covariation of the relative growth rate change 411 γ and the relative lag time change ω for a single fixed mu-

$$\rho_{\text{fixed}} \approx \frac{\langle \gamma \omega \rangle_{\text{fixed}} - \langle \gamma \rangle_{\text{fixed}} \langle \omega \rangle_{\text{fixed}}}{\sqrt{(\langle \gamma^2 \rangle_{\text{fixed}} - \langle \gamma \rangle_{\text{fixed}}^2)(\langle \omega^2 \rangle_{\text{fixed}} - \langle \omega \rangle_{\text{fixed}}^2)}},$$
(10)

where $\langle \cdot \rangle_{\text{fixed}}$ is an average over the distribution of sin-414 gle fixed mutations (Supplementary Methods Sec. IX). We can explicitly calculate this quantity in the SSWM regime, which confirms that it is positive for uncorrelated mutational effects with uniform or Gaussian distributions (Supplementary Methods Sec. XI).

However, in evolution experiments we typically observe 420 populations at a particular snapshot in time, such that the populations may have a variable number of fixed mu-422 tations but the same number of total mutations that arose and either fixed or went extinct (since the number of total arising mutations is very large, we neglect its fluc-425 tuation across populations). Interestingly, the variation in number of fixed mutations at a snapshot in time causes the distribution of growth rates and lag times across pop-428 ulations to stretch into a negative correlation; this is an 429 example of Simpson's paradox from statistics [46]. Fig-430 ure 5a shows this effect schematically, while Fig. 5d,e 431 show explicit results from simulations. An intuitive way 432 to understand the evolved negative correlation is to ap-433 proximate the effects of all fixed mutations as determin-We now turn to investigating how the covariation be- 434 istic, so that each fixed mutation increases the average tween traits evolves. We have generally assumed that in- 435 growth rate and decrease the average lag time by the dividual mutations have uncorrelated effects on different 436 same amount. Therefore populations with a higher aver-

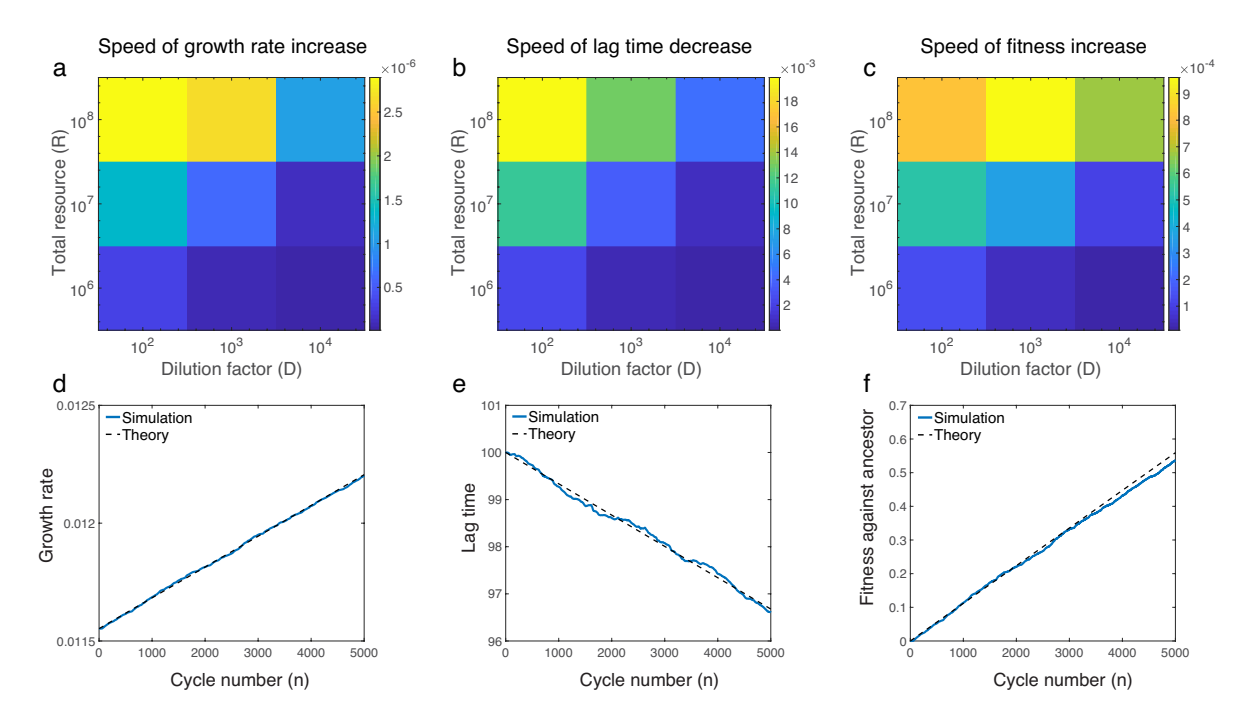


FIG. 4. Speed of adaptation. The average per-cycle adaptation speed of (a) the average growth rate, (b) the average lag time, and (c) the fitness relative to the ancestral population as functions of the dilution factor D and total amount of resources R. The adaptation speeds are averaged over growth cycles and independent populations. (d) The average growth rate, (e) the average lag time, and (f) the fitness relative to the ancestral population as functions of the number n of growth cycles. The dilution factor is $D = 10^4$ and the total resource is $R = 10^7$, so the population is in the SSWM regime. The blue solid lines are simulation results, while the dashed lines show the mathematical predictions in Eq. 8. All panels show averages over 500 independent simulated populations, with mutations randomly arising from a uniform distribution p_{mut} with $-0.02 < \gamma < 0.02$, $-0.05 < \omega < 0.05$, and $-0.02 < \delta < 0.02$.

437 age growth rate must have a larger number of fixed muta- 459 ter regimes of our simulations (Fig. S6a,b,c). However, 438 tions and thus also a shorter average lag time, leading to 460 the signs of the correlations can indeed change depend-439 a negative correlation between the average growth rates 461 ing on the underlying distribution of mutational effects 440 and the average lag times. In the Supplementary Meth-462 $p_{\rm mut}(\gamma,\omega,\delta)$. For example, in the Supplementary Meth-441 ods (Sec. X), we calculate this evolved Pearson correla-463 ods we explore the effects of varying the mean mutational 442 tion coefficient across populations in the SSWM regime 464 effects (Fig. S6d) — e.g., whether an average mutation 443 to be approximately

$$\rho_{\text{evo}} \approx \frac{\langle \gamma \omega \rangle_{\text{fixed}}}{\sqrt{\langle \gamma^2 \rangle_{\text{fixed}} \langle \omega^2 \rangle_{\text{fixed}}}}.$$
(11)

444 That is, the correlation of traits across populations with 445 multiple mutations is still a function of the distribution 446 of single fixed mutations, but it is not equal to the corre-447 lation of single fixed mutations (Eq. 10). In the Supple-448 mentary Methods (Sec. XI) we explicitly calculate $\rho_{\rm evo}$ in 449 the SSWM regime for uncorrelated uniform and Gaussian 450 distributions of mutational effects, which shows that it is 451 negative. Furthermore, we prove that it must always be 452 negative for any symmetric and uncorrelated distribution $p_{\text{mut}}(\gamma,\omega)$ (Supplementary Methods Sec. IX).

The predicted correlations in Eqs. 10 and 11 quantita-455 tively match the simulations well in the SSWM regime 456 (Fig. 5c,e). While they are less accurate outside of the 457 SSWM regime, they nevertheless still produce the cor-458 rect sign of the evolved correlation within the parame-

465 has positive, negative, or zero effect on the growth rate 466 — as well as the intrinsic mutational correlation between 467 the relative growth rate change and the relative lag time (11) 468 change (Fig. S6e).

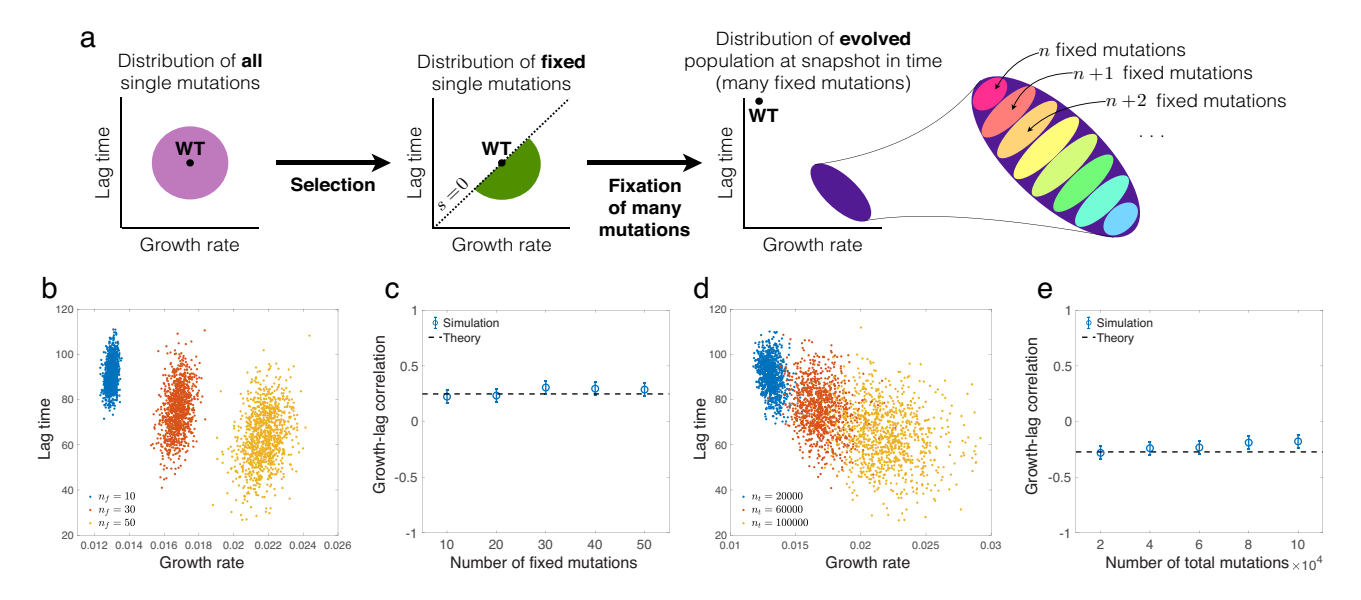


FIG. 5. Evolved patterns of covariation among growth traits. (a) Schematic of how selection and fixation of multiple mutations shape the observed distribution of traits. The sign of the Pearson correlation coefficient between the average growth rate and lag time depends on whether we consider an ensemble of populations with the same number of fixed mutations or the same number of total mutation events. (b) Distribution of average growth rate and lag time for 1000 independent populations with the same number of fixed mutations. Each color corresponds to a different number of fixed mutations (n_f) indicated in the legend. (c) Pearson correlation coefficient of growth rate and lag time for distributions in panel (b) as a function of the number of fixed mutations. The dashed line is the prediction from Eq. 10. (d) Same as (b) except each color corresponds to a set of populations at a snapshot in time with the same number of total mutation events. Each color corresponds to a different number of total mutations events (n_t) indicated in the legend. (e) Same as (c) but for the set of populations shown in (d). The dashed line is the prediction from Eq. 11. In (c) and (e) the error-bars represent 95% confidence intervals. In (b-e) we simulate the SSWM regime by introducing random mutations one-by-one and determining their fixation from Eq. 5 with $D=10^3$.

III. DISCUSSION

We have investigated a model of microbial evolution under serial dilution, which is both a common protocol for laboratory evolution experiments [1, 6, 31, 47, 48] as well as a rough model of evolution in natural environments with feast-famine cycles. While there has been extensive work to model population and evolutionary dynamics in these conditions [2, 35, 36, 38, 45], these models have largely neglected the physiological links connecting mutations to selection. However, models that explicitly incorporate these features are necessary to interpret experimental evidence that mutations readily generate variation in multiple cellular traits, and that this variation is important to adaptation [17–20]. Wahl and Zhu [22] determined the relative fixation probabilities of mutations on different traits and the effects of mutation occurrence time and dilution factor, but the role of pleiotropy and evolutionary dynamics over many mutations were not 486 considered. 487

In this paper, we have studied a model where mutations can affect three quantitative growth traits — the lag time, the exponential growth rate, and the yield (Fig. 1a) 517 492 bial populations. In particular, we have derived a simple 519 which requires that the bottleneck population size N_0 493 expression (Eq. 3) for the selection coefficient of a muta-520 fluctuates as the population evolves. In contrast, previ-

495 environmental parameter, the dilution factor D. While 496 previous work showed that this particular form of the selection coefficient determines the fixation probability of a single mutation in the SSWM regime [23], here we show that this holds even in the presence of clonal interfer-500 ence (Fig. 2c,d,e,f), which appears to be widespread in 501 laboratory evolution experiments [9, 28, 49]. Our result is therefore valuable for interpreting the abundant ex-503 perimental data on mutant growth traits. We have also 504 calculated the adaptation rates of growth traits per cycle 505 in the SSWM regime, which turn out to increase with 506 the amount of resource R and decrease with the dilution factor D. These results are confirmed by numerical simulations and remain good predictions even outside of the SSWM regime. Furthermore, some of these results are 510 independent of the specific form of the selection coeffi-511 cient (Eq. 3), namely the fact that the fixation probabil-512 ity depends only on the selection coefficient (with other 513 population parameters besides the mutant traits being 514 held fixed) even in the clonal interference regime, and 515 the expressions for the correlation coefficients of traits between populations (Eqs. 10 and 11).

An important difference with the previous work on this since these three traits are widely measured for micro- 518 model is that here we used a fixed dilution factor D, 494 tion in terms of its effects on growth and lag and a single 521 ous work used a fixed N_0 and variable D [23, 24]. We ob-

522 served two important differences between these regimes. 580 but recent work by Gomez et al. [51] provides insight into lection by varying either the total amount of resources 587 within populations. $_{530}$ R or the fixed bottleneck size N_0 . However, when the $_{588}$ $_{542}$ and lag traits of the strains to follow an exact constraint $_{600}$ theory, which suggests there should be tradeoffs between set by D (Supplementary Methods Sec. III).

flates both the underlying supply of variation from mutanegative correlation between two traits from evolved pop- 620 these issues [33]. ulations is insufficient to infer whether that correlation is due to a physiological constraint on mutations (e.g., 565 mutations cannot improve both traits simultaneously) or due to a selective constraint (e.g., selection favors specialization in one trait or another).

These questions, of course, have been the foundation of 622 578 bial populations in this regime. In the present study, we 632 time correlation presented in the Supplementary Meth-⁵⁷⁹ focus on between-population covariation in growth traits, ⁶³³ ods.

First, in the case of fixed N_0 and variable D, the fold- 581 the case of within-population covariation. They showed change of the population during a single growth cycle, 582 that a tradeoff across individuals within a population which is approximately $R\bar{Y}/N_0$ [23], determines the rela- 583 evolves between two quantitative traits under positive, tive selection between growth and lag, since it determines 554 additive selection; this suggests that while growth rate how long the population undergoes exponential growth. 585 and lag time will be negatively correlated across popu-Therefore one can experimentally tune this relative se-586 lations (Fig. 5d,e), they should be positively correlated

Microbial growth traits should indeed be an ideal setdilution factor D is fixed, the population fold-change is 589 ting for this approach due to abundant data, but conalways constrained to exactly equal D and therefore D 590 clusions on the nature of trait covariation have remained alone determines the relative selection on growth and lag $_{591}$ elusive. Physiological models have predicted a negative (Eq. 3). The second difference is that, with fixed N_0 and p_{92} correlation between growth rate and lag time across genovariable D, the selection coefficient depends explicitly on 593 types [52, 53], while models of single-cell variation in lag the effective yield \bar{Y} and is therefore frequency-dependent $_{594}$ times also suggests there should be a negative correla-(Supplementary Methods Sec. II), which enables the pos- 595 tion at the whole-population level [54]. However, exsibility of stable coexistence between two strains [23, 24]. 596 perimental evidence has been mixed, with some stud-However, for the fixed D case, the frequency dependence $_{597}$ ies finding a negative correlation [13, 16], while others of \bar{Y} is exactly canceled by N_0 (Eq. 4). Therefore there is 598 found no correlation [10, 11, 14]. Studies of growth-yield only neutral coexistence in this case, requiring the growth $_{599}$ correlations have long been motivated by r/K selection 601 growth rate and yield [55]. For instance, metabolic mod-A major result of our model is a prediction on the 602 els make this prediction [56-58]. However, experimental evolution of covariation between growth traits. In par- 603 evidence has again been mixed, with some data showticular, we have shown that correlations between traits 604 ing a tradeoff [26, 59, 60], while others show no correlacan emerge from selection and accumulation of multiple 605 tion [15, 18, 19, 61] or even a positive correlation [11, 47]. mutations even without an intrinsic correlation between 606 Some of this ambiguity may have to do with dependence traits from individual mutations (Figs. 5 and S6). We 607 on the environmental conditions [19] or the precise definihave also shown that selection alone produces no corre- 608 tion of yield. We define yield as the proportionality conlation between growth and yield, in the absence of corre- 609 stant of population size to resource (Eq. 1) and neglect lated mutational effects (Figs. 2b and 3e). This is impor- 610 any growth rate dependence on resource concentration. tant for interpreting evolved patterns of traits in terms 611 Under these conditions, we predict no direct selection of selective or physiological tradeoffs. Specifically, it em- $_{612}$ on yield, which means that the only way to generate a phasizes that the evolved covariation between traits con- 613 correlation of yield with growth rate is if the two traits 614 are constrained at the physiological level, so that mutations as well as the action of selection and other aspects 615 tional effects are correlated. In such cases yield could of population dynamics (e.g., genetic drift, spatial struc- 616 evolve but only as a spandrel [62, 63]. Ultimately, we ture, recombination), and therefore it is difficult to make $_{617}$ believe more precise single-cell measurements of these clear inferences about either aspect purely from the out- 618 traits, both across large unselected mutant libraries as come of evolution alone. For example, simply observing a 619 well as evolved strains, are necessary to definitively test

ACKNOWLEDGMENTS

MM was supported by an F32 fellowship from the US quantitative trait genetics [50]. Historically this field has 623 National Institutes of Health (GM116217) and an Amemphasized polymorphic populations with abundant re- 624 bizione grant from the Swiss National Science Foundacombination as are applicable to plant and animal breed- 625 tion (PZ00P3_180147). AA was supported by NSF CAing. However, this regime is quite different from micro- 626 REER grant 1752024 and the Harvard Dean's Competbial populations which, at least under laboratory con- 627 itive Fund. AA and JL thank support from Harvard's ditions, are often asexual and dominated by linkage be- 628 MRSEC (DMR-1420570). We thank Christine Jacobstween competing mutations [9, 28, 49]. We therefore need 629 Wagner for kindly sharing the data of single-gene delea quantitative description of both between-population as 650 tions of E. coli, and we thank Yipei Guo for suggesting well as within-population covariation of traits of micro- 631 the proof of the sign of the evolved growth rate and lag [1] S. F. Elena and R. E. Lenski, "Evolution experiments 694 with microorganisms: the dynamics and genetic bases of adaptation," Nat Rev Genet 4, 457-469 (2003).

634

635

636

637

638

641

645

646

647

648

649

650

651

652

653

654

655

656

657

661

662

663

664

665

- M. M. Desai, "Statistical questions in experimental evolution," J Stat Mech 2013, P01003 (2013).
- J. E. Barrick and R. E. Lenski, "Genome dynamics dur-639 ing experimental evolution," Nat Rev Genet 14, 827-839 640
- Michael J. Wiser, Noah Ribeck, and Richard E. Lenski, 642 "Long-term dynamics of adaptation in asexual popula-643 tions," Science (2013).
 - S. Kryazhimskiy, D. P. Rice, E. R. Jerison, and M. M. 705 Desai, "Global epistasis makes adaptation predictable 706 [19] despite sequence-level stochasticity," Science 344, 1519-707 1522 (2014).
 - S. F. Levy, J. R. Blundell, S. Venkataram, D. A. Petrov, 709 D. S. Fisher, and G. Sherlock, "Quantitative evolution-710 [20] ary dynamics using high-resolution lineage tracking," Na-711 ture **519**, 181–186 (2015).
 - S. Wielgoss, J. E. Barrick, O. Tenaillon, S. Cruveiller, 713 B. Chane-Woon-Ming, C. Médigue, R. E. Lenski, and 714 D. Schneider, "Mutation rate inferred from synonymous 715 substitutions in a long-term evolution experiment with 716 Escherichia coli," G3 1, 183–186 (2011).
- J. E. Barrick, D. S. Yu, S. H. Yoon, H. Jeong, T. K. Oh, 718 658 D. Schneider, R. E. Lenski, and J. F. Kim, "Genome 719 659 evolution and adaptation in a long-term experiment with 720 660 Escherichia coli," Nature **461**, 1243–1247 (2009).
 - G. I. Lang, D. P. Rice, M. J. Hickman, E. Sodergren, 722 G. M. Weinstock, D. Botstein, and M. M. Desai, "Per- 723 [24] vasive genetic hitchhiking and clonal interference in forty 724 evolving yeast populations," Nature **500**, 571–574 (2013). 725
- I. Levin-Reisman, O. Gefen, O. Fridman, I. Ronin, 726 D. Shwa, H. Sheftel, and N. Q. Balaban, "Automated 727 667 imaging with ScanLag reveals previously undetectable 728 668 bacterial growth phenotypes," Nat Methods 7, 737–739 729 [26] 669 (2010).670
- [11] J. Warringer, E. Zörgö, F. A. Cubillos, A. Zia, A. Gju-731 671 vsland, J. T. Simpson, A. Forsmark, R. Durbin, S. W. 732 672 Omholt, E. J. Louis, G. Liti, A. Moses, and A. Blomberg, 733 673 "Trait variation in yeast is defined by population his-674 tory," PLOS Genet 7, e1002111 (2011). 675
- M. Zackrisson, J. Hallin, L.-G. Ottosson, P. Dahl, 736 676 E. Fernandez-Parada, E. Ländström, L. Fernandez- 737 677 Ricaud, P. Kaferle, A. Skyman, S. Stenberg, S. Omholt, 738 678 U. Petrovic, J. Warringer, and A. Blomberg, "Scan-o-679 matic: High-resolution microbial phenomics at a massive 680 scale," G3 6, 3003-3014 (2016). 681
- N. Ziv, B. M. Shuster, M. L. Siegal, and D. Gresham, 682 "Resolving the complex genetic basis of phenotypic vari-683 ation and variability of cellular growth," Genetics 206, 684 1645–1657 (2017). 685
- B. V. Adkar, M. Manhart, S. Bhattacharyya, J. Tian, 686 687 M. Musharbash, and E. I. Shakhnovich, "Optimization of lag phase shapes the evolution of a bacterial enzyme," 688 Nat Ecol Evol 1, 0149 (2017). 689
- J. M. Fitzsimmons, S. E. Schoustra, J. T. Kerr, and [15]690 R. Kassen, "Population consequences of mutational 691 692 events: effects of antibiotic resistance on the r/K tradeoff," Evol Ecol **24**, 227–236 (2010).

- [16] N. Ziv, M. L. Siegal, and D. Gresham, "Genetic and Nongenetic Determinants of Cell Growth Variation Assessed by High-Throughput Microscopy," Molecular Biology and Evolution 30, 2568-2578 (2013).
- F. Vasi, M. Travisano, and R. E. Lenski, "Long-term 698 experimental evolution in Escherichia coli. II. changes in life-history traits during adaptation to a seasonal environment," Am Nat 144, 432-456 (1994).
- M. Novak, T. Pfeiffer, R. E. Lenski, U. Sauer, and [18] 702 S. Bonhoeffer, "Experimental tests for an evolutionary trade-off between growth rate and yield in E. coli," Am Nat 168, 242–251 (2006).
 - C. Reding-Roman, M. Hewlett, S. Duxbury, F. Gori, I. Gudelj, and R. Beardmore, "The unconstrained evolution of fast and efficient antibiotic-resistant bacterial genomes," Nat Ecol Evol 1, 0050 (2017).
 - Y. Li, S. Venkataram, A. Agarwala, B. Dunn, D. A. Petrov, G. Sherlock, and D. S. Fisher, "Hidden complexity of veast adaptation under simple evolutionary conditions," Current Biology 28, 515-525 (2018).
 - H. L. Smith, "Bacterial competition in serial transfer culture," Math Biosci 229, 149-159 (2011).
 - L. M. Wahl and A. D. Zhu, "Survival probability of beneficial mutations in bacterial batch culture," Genetics 200, 309-320 (2015).
 - M. Manhart, B. V. Adkar, and E. I. Shakhnovich, "Trade-offs between microbial growth phases lead to frequency-dependent and non-transitive selection," Proc R Soc B **285**, 20172459 (2018).
 - M. Manhart and E. I. Shakhnovich, "Growth tradeoffs produce complex microbial communities on a single limiting resource," Nat Commun 9, 3214 (2018).
 - [25] J. Lin and A. Amir, "The effects of stochasticity at the single-cell level and cell size control on the population growth," Cell Systems 5, 358–367 (2017).
 - J.-N. Jasmin and C. Zeyl, "Life-history evolution and density-dependent growth in experimental populations of yeast," Evolution **66**, 3789–3802 (2012).
 - L.-M. Chevin, "On measuring selection in experimental evolution," Biol Lett 7, 210-213 (2011).
- B. H. Good, M. J. McDonald, J. E. Barrick, R. E. Lenski, 734 and M. M. Desai, "The dynamics of molecular evolution over 60,000 generations," Nature **551**, 45–50 (2017).
 - S. E. Finkel, "Long-term survival during stationary phase: evolution and the gasp phenotype," Nature Reviews Microbiology 4, 113 (2006).
- [30] Sarit Avrani, Evgeni Bolotin, Sophia Katz, and Ruth 740 Hershberg, "Rapid genetic adaptation during the first four months of survival under resource exhaustion," Molecular Biology and Evolution 34, 1758–1769 (2017).
- R. E. Lenski, M. R. Rose, S. C. Simpson, and S. C. 744 Tadler, "Long-term experimental evolution in escherichia coli. i. adaptation and divergence during 2,000 generations," The American Naturalist 138, 1315–1341 (1991).
- [32]G. Chevereau, M. Dravecká, T. Batur, A. Guvenek, D. H. 748 Ayhan, E. Toprak, and T. Bollenbach, "Quantifying the determinants of evolutionary dynamics leading to drug resistance," PLoS Biol 13, e1002299 (2015).
- 752 Manuel Campos, Sander K Govers, Irnov Irnov, Genevieve S Dobihal, François Cornet, and Christine Jacobs-Wagner, "Genomewide phenotypic analysis

753

754

of growth, cell morphogenesis, and cell cycle events in 804 escherichia coli," Mol Syst Biol 14, e7573 (2018).

805

808

810

817

819

820

842

843

844

845

J. H. Gillespie, "Molecular evolution over the mutational 757 landscape," Evolution 38, 1116–1129 (1984). 758 807

755

756

778

781

- Lindi M Wahl and Philip J Gerrish, "The probability that 759 beneficial mutations are lost in populations with periodic 809 760 bottlenecks," Evolution 55, 2606–2610 (2001). 761
- Y. Guo, M. Vucelja, and A. Amir, "Stochastic tunneling 811 [51] 762 across fitness valleys can give rise to a logarithmic long-763 term fitness trajectory," Sci Adv 5, eaav3842 (2019). 764
- J. F. Crow and M. Kimura, An Introduction to Pop-765 ulation Genetics Theory (Harper and Row, New York, 766 767
- P. J. Gerrish and R. E. Lenski, "The fate of competing 768 beneficial mutations in an asexual population," Genetica 818 [53] 769 **102**, 127 (1998). 770
- Michael M Desai and Daniel S Fisher, "Beneficial 771 mutation—selection balance and the effect of linkage on 772 positive selection," Genetics 176, 1759–1798 (2007). 773
- [40]Stephan Schiffels, Gergely J. Szöllősi, Ville Mustonen, 774 and Michael Lässig, "Emergent neutrality in adaptive 775 asexual evolution," Genetics 189, 1361–1375 (2011). 776
- Benjamin H. Good, Igor M. Rouzine, Daniel J. Balick, 777 Oskar Hallatschek, and Michael M. Desai, "Distribution of fixed beneficial mutations and the rate of adapta-779 tion in asexual populations," Proceedings of the National 780 Academy of Sciences 109, 4950–4955 (2012).
- Daniel S Fisher, "Asexual evolution waves: fluctuations 831 42] 782 and universality," Journal of Statistical Mechanics: The-783 ory and Experiment 2013, P01011 (2013). 784
- 785 ous passengers in adapting populations," Genetics 198, 835 786 1183–1208 (2014). 787
- 788 Principles of population genetics, Vol. 116 (Singuer asso-789 ciates Sunderland, 1997). 790
- [45]791 and Anton Wakolbinger, "Modelling and simulating 841 792 lenskis long-term evolution experiment," Theoretical 793 Population Biology 127, 58 – 74 (2019). 794
- E. H. Simpson, "The interpretation of interaction in con-795 tingency tables," Journal of the Royal Statistical Society: 796 Series B (Methodological) 13, 238–241 (1951). 797
- L. S. Luckinbill, "r and K selection in experimental pop-798 ulations of Escherichia coli," Science 202, 1201-1203 848 799 (1978).800
- Karin E. Kram, Christopher Geiger, Wazim Mohammed [48]801 Ismail, Heewook Lee, Haixu Tang, Patricia L. Foster, 851 802 and Steven E. Finkel, "Adaptation of escherichia coli to 852 [63] 803

- long-term serial passage in complex medium: Evidence of parallel evolution," mSystems 2 (2017).
- 806 [49] G. I. Lang, D. Botstein, and M. M. Desai, "Genetic variation and the fate of beneficial mutations in asexual populations," Genetics 188, 647–661 (2011).
 - M. Lynch and B. Walsh, Genetics and Analysis of Quantitative Characters (Sinauer, Sunderland, MA, 1998).
- K. Gomez, J. Bertram, and J. Masel, "Directional selection rather than functional constraints can shape the G matrix in rapidly adapting asexuals," Genetics 211, 813 814 715-729 (2019).
- 815 [52] J. Baranyi and T. A. Roberts, "A dynamic approach to predicting bacterial growth in food," Int J Food Microbiol 23, 277–294 (1994).
 - Y. Himeoka and K. Kaneko, "Theory for transitions between exponential and stationary phases: Universal laws for lag time," Phys Rev X 7, 021049 (2017).
 - J. Baranyi, "Comparison of stochastic and deterministic concepts of bacterial lag," J Theor Biol 192, 403-408 (1998).
- 824 [55] D. Reznick, M. J. Bryant, and F. Bashey, "r- and Kselection revisited: The role of population regulation in life-history evolution," Ecology 83, 1509–1520 (2002).
- T. Pfeiffer, S. Schuster, and S. Bonhoeffer, "Coopera-827 tion and competition in the evolution of ATP-producing pathways," Science 292, 504-507 (2001).
- R. C. MacLean, "The tragedy of the commons in mi-830 [57] crobial populations: insights from theoretical, comparative and experimental studies," Heredity 100, 471-477 832 (2007).
- [43] Benjamin H. Good and Michael M. Desai, "Deleteri- 834 [58] J. R. Meyer, I. Gudelj, and R. Beardmore, "Biophysical mechanisms that maintain biodiversity through tradeoffs." Nat Commun 6, 6278 (2015).
- [44] Daniel L Hartl, Andrew G Clark, and Andrew G Clark, 837 [59] J.-N. Jasmin, M. M. Dillon, and C. Zevl, "The vield of experimental yeast populations declines during selec-838 tion," Proc R Soc B 279, 4382-4388 (2012). 839
 - Ellen Baake, Adrin Gonzlez Casanova, Sebastian Probst, 840 [60] H. Bachmann, M. Fischlechner, I. Rabbers, N. Barfa, F. B. dos Santos, D. Molenaar, and Bas Teusink, "Availability of public goods shapes the evolution of competing metabolic strategies," Proc Natl Acad Sci USA 110, 14302-14307 (2013).
 - G. J. Velicer and R. E. Lenski, "Evolutionary trade-offs under conditions of resource abundance and scarcity: Experiments with bacteria," Ecology **80**, 1168–1179 (1999).
 - [62]S. J. Gould and R. C. Lewontin, "The spandrels of San Marco and the Panglossian paradigm: A critique of the adaptationist programme," Proc R Soc B 205, 581–598 (1979).
 - A. Amir, "Point of view: Is cell size a spandrel?" eLife **6**, e22186 (2017).